# Tautomeric Forms of Azolide Anions: Vertical Electron Detachment Energies and Dyson Orbitals

**Junia Melin,[†] Raman K. Singh,[‡] Manoj K. Mishra,*[,‡] and J. V. Ortiz*[,†]**

*Department of Chemistry and Biochemistry, Auburn University, Auburn, Alabama 36849-5312, and Department of Chemistry, Indian Institute of Technology, Bombay, Powai, Mumbai 400 076, India*

*Received: July 13, 2007; In Final Form: September 10, 2007*

Several decouplings of the electron propagator, including the relatively new P3+ approximation for the self-energy, have been used to calculate vertical electron detachment energies of tautomeric forms of closed-shell, pentagonal, aromatic anions in which ring carbons without bonds to hydrogens appear. This study extends previous work in which the most stable forms of anionic, five-member rings with one to five nitrogens were considered. Whereas the lowest electron detachment energies sometimes are assigned by Koopmans's theorem results to $\pi$ orbital vacancies, electron propagator calculations always obtain $\sigma$ orbital vacancies for the ground states of the doublet radicals. Higher electron detachment energies that correspond to excited doublets with $\pi$ vacancies also are presented. The predicted transition energies are in good agreement with low-intensity peaks in recent anion photoelectron spectra that have been assigned to less stable, tautomeric forms of these anions.

## I. Introduction

The family of five-member aromatic rings containing one or more nitrogen atoms has attracted much attention for its pharmacological utility as constituents of important drugs such as anastrozole, estazolam, and triazolam. These polynitrogen molecules, called azoles, also have promise as high-energy density materials for rocket propellants and as corrosion inhibitors. Because electron binding energies and other thermochemical properties are important indices of chemical reactivity, detailed experimental and computational studies on some of these anions and their related radicals have appeared in recent years.[1−15]

Photoelectron spectra of pyrrolide,[10] imidazolide,[11] and pyrazolide[12] anions have been reported. Detailed theoretical studies of the latter anion and vibronic coupling in the corresponding radical also have appeared.[13] Calculated N−H acidity values and other thermochemical information in refs 12, 13, and 15 are in good agreement with data inferred from experiment in the first two of these articles. In the published spectra, the most intense features pertain to the standard structures, where there are no carbon atoms without bonds to hydrogens. However, for imidazolide and pyrazolide, the method of synthesis involves the reaction of a precursor molecule with a strong base ($OH^-$), which has the ability to remove protons from carbon atoms, resulting in the production of less stable tautomeric forms of the anions. These species reportedly give rise to less intense features in the photoelectron spectrum, which occur at lower electron binding energies. In the analysis of these observations, care has been taken to distinguish hot bands pertaining to the most stable isomer from those which belong to less stable forms of the anions.

In an earlier paper,[14] we presented a theoretical study of electronic structure and electron detachment energies for pentagonal aromatic anions, starting with the pyrrolide and imidazolide anions and progressing to the pentazolide anion by a systematic substitution of CH groups by nitrogen atoms. Whereas some of these structures are well-known (such as pyrrolide and imidazolide), experimental proof only for the existence of $N_5^-$ has been reported relatively recently.[6] The need for accurate predictions on still unreported species and the variety of electronic structure patterns displayed by them have stimulated us to calculate electron detachment energies of these anions with electron propagator theory (EPT).[16−18] Electron propagator methods are a versatile and reliable means of determining vertical electron attachment and detachment energies of molecules.[19−22] They include electron correlation and orbital relaxation effects and generate Dyson orbitals, which provide reliable explanations for structural changes that accompany electron attachment and detachment processes.

We presently extend our previous study[14] on polynitrogen compounds to tautomeric isomers of the azolides by predicting their electron detachment energies and providing an analysis of the corresponding Dyson orbitals. Changes in the latter functions that accompany proton transfers from one atom to another and their energetic consequences will be considered. These results should help in the interpretation of photoelectron spectra of novel azolides, especially when the question of isomeric forms of the anions arises.[10−14]

## II. Theory and Methods

EPT is well-established,[16−22] and only a minimal outline of its features is offered here. The Dyson equation governing all electron propagator decouplings may be rewritten in the form of one-electron equations such that

$$[\hat{f} + \hat{\Sigma}(\epsilon_i)]\phi_i^{\text{Dyson}}(x) = \epsilon_i \phi_i^{\text{Dyson}}(x) \qquad (1)$$

where $\hat{f}$ is the one-electron Hartree−Fock (HF) operator and $\hat{\Sigma}$ $(\epsilon)$ is an energy-dependent nonlocal operator, the so-called self-energy. This operator describes electron correlation and

* Corresponding authors. E-mail: ortiz@auburn.edu (J.V.O.) and mmishra@iitb.ac.in (M.K.M.).
[†] Auburn University.
[‡] Indian Institute of Technology.

10.1021/jp075496m CCC: $37.00 
Published on Web 11/15/2007

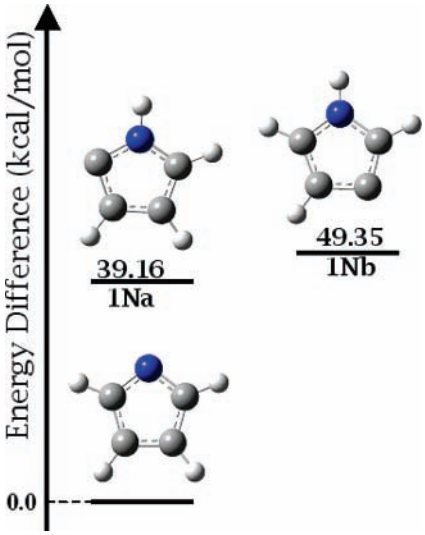


**Figure 1.** Energy differences for pyrrolide isomers.

orbital relaxation effects that are neglected by the HF operator, $\hat{f}$. Eigenfunctions of eq 1 are the Dyson orbitals, $\phi_i^{\text{Dyson}}$. For vertical electron detachment processes, the Dyson orbitals are given by

$$\phi_i^{\text{IP,Dyson}}(x_N) = \sqrt{N} \int \Psi_N(x_1,x_2,x_3,...,x_N)\Psi^*_{i,N-1} (x_1,x_2,x_3,...,x_{N-1})\, dx_1\, dx_2 ...\, dx_{N-1} \quad (2)$$

Here, $\Psi_N(x_1...,x_N)$ is the wavefunction for the $N$-electron, initial state and $\Psi_{i,N\pm1}(x_1...,x_{N\pm1})$ is the wavefunction for the $i$th final state with $N \pm 1$ electrons. In both expressions, $x_j$ represents the space−spin coordinates of electron $j$. The eigenvalues, $\epsilon_i$, of the Dyson equation correspond to electron binding energies of the molecular system. By using perturbative arguments, one may justify neglect of off-diagonal matrix elements of the self-energy operator in the HF basis. This leads to the simpler quasi-particle expression, also called the diagonal approximation. Thus, the electron binding energies in the quasi-particle approximation read $\epsilon_i^{\text{HF}} + \Sigma_{ii}(E) = E$, where $\epsilon_i^{\text{HF}}$ is the $i$th canonical, HF orbital energy. All EPT methods used in this paper are based on this approximation, including the recently developed P3+ method.[23] The pole strength, $p_i$, is a good indicator of the qualitative validity of this approximation. Because the pole strength is defined by

$$p_i = \int |\phi_i^{\text{Dyson}}(x)|^2\, dx \quad (3)$$

the Dyson orbital within the diagonal approximation is simply proportional to a normalized, canonical HF orbital such that

$$\phi_i^{\text{Dyson}}(x) = \sqrt{p_i}\psi_i^{HF}(x) \quad (4)$$

Thus, the pole strength takes values between zero and unity. If the ionization process is well-described by a Koopmans (frozen-orbital) picture, pole strengths are very close to 1.0. When pole strengths are less than 0.8, non-diagonal analysis of energy poles is required. All pole strengths in this work exceed 0.8. Those that are below 0.85 are less reliable and therefore the corresponding electron binding energies are denoted by footnotes in the tables.

Geometry optimizations and frequency calculations for the series of nitrogen-containing molecules presented here were performed at the MP2/6-311++(2df,2p) level with Gaussian03.[24] All structures have a plane of symmetry and positive, real frequencies. Electron propagator calculations were performed with the same basis set, and a modified version of Gaussian03 was used to obtain the P3+ values. The latter results follow the same trends that characterized other EPT methods and closely resemble OVGF[25] results. The Dyson orbital pictures presented in the tables were created with GaussView, and an isosurface value of 0.1 was used to produce the figures.

## III. Results and Discussion

Figures 1−4 show the relative energies for each of the presently studied isomers relative to those considered in the previous study[14] where the origin of the energy scale corresponds to the total energy of the most stable anion. As can be seen from Figure 1, two pyrrolide isomers are separated by ∼10 kcal/mol. The energy gap between the two isomeric structures and the most stable form of the pyrrolide anion is even larger. The lower energy of these two tautomeric configurations occurs

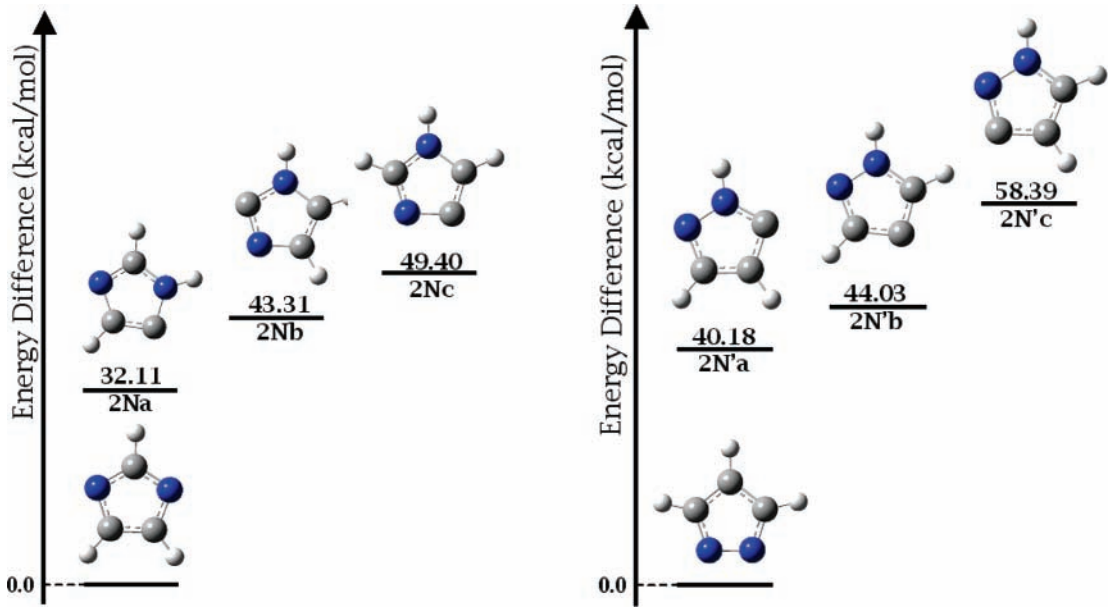


**Figure 2.** Energy differences for imidazolide (left) and pyrazolide (right) isomers.

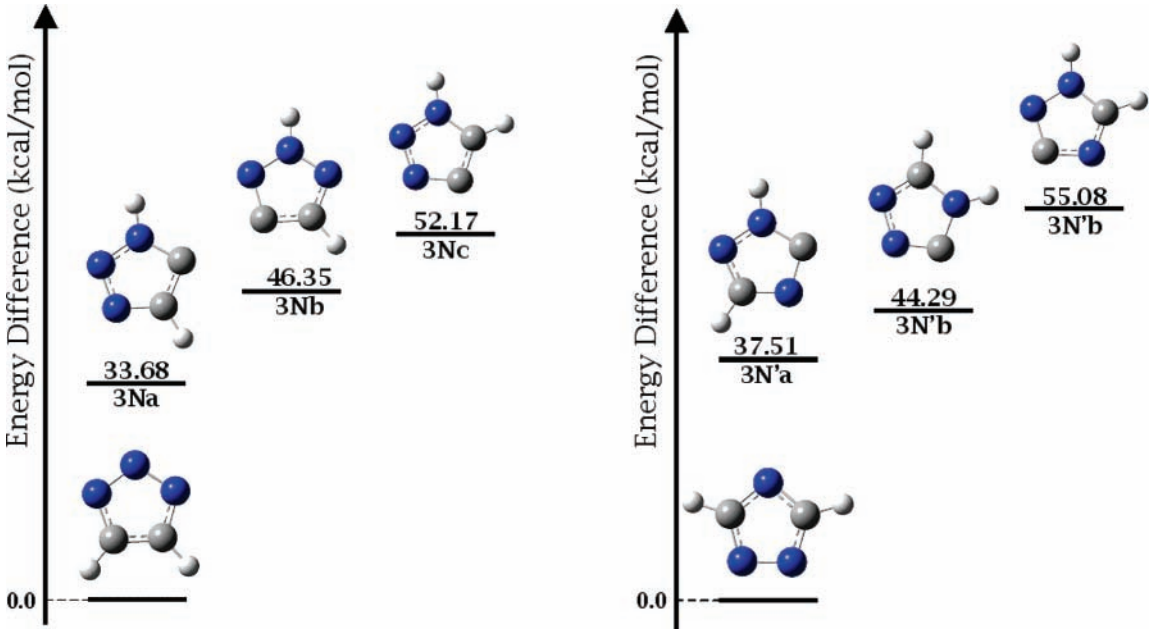


**Figure 3.** Energy differences for triazolides isomers.

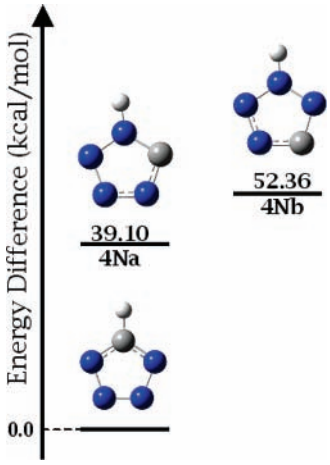


**Figure 4.** Energy differences for tetrazolide isomers.

when the carbon that is missing a hydrogen is next to the nitrogen atom.

Results for the two diazolides are shown in Figure 2. The energy difference between imidazolide and the first isomer is 32.11 kcal/mol. This value might be compared with the difference in reaction enthalpies reported by Gianola et al. between the 1- and 5-imidazolides (38.2 kcal/mol).[11] Note however that their calculations (B3LYP/6-311++G(d,p)) differ from ours (MP2/6-311++G(2df,2p)) in method and basis set. The optimized geometry for this isomer is in good agreement with previous work as well.[11] Differences in bond lengths are not larger than 0.01 Å, whereas discrepancies in angles are less than 0.7°. When the two nitrogen atoms are next to each other, the energy differences with respect to the most stable structure increase ($\Delta E = 40.18$ kcal/mol). However, this energy is much larger than the enthalpy differences in reference 13 (29.6 kcal/mol). Comparison of optimized geometries between the 5-pyrazolide in a previous report (see Table 3 in reference 13) with our 2N′a structure shows good agreement. Again, differences in bond lengths are within 0.01 Å and angle differences are less than 0.8°.

Figure 3 depicts the energy profile for triazolide isomers. Just as in the case of diazolides, there are three isomeric configurations for each stable anion. Even though the structure with nonadjacent nitrogen atoms is energetically preferred, the higher and lower isomers' energies differ by ∼18 kcal/mol in both cases.

The relative energy profile for tetrazolide isomers is displayed in Figure 4. As with the pyrrolide structures of Figure 1, only two isomers are found, and the lower in energy is 39 kcal/mol above the most stable nuclear configuration.

Vertical electron detachment energies (VEDEs) and Dyson orbitals, obtained with various electron propagator approximations for each series of isomers, are presented in Tables 1 to 4, which summarize the results for the first three binding energies. Koopmans's theorem (KT) values listed in the first row represent in each case the canonical orbital energies obtained with a standard HF/6-311++G(2df,2p) calculation. The following rows correspond to EPT methods, including the recently developed P3+ approximation.

Table 1 shows that the KT orbital symmetry ordering (A″, A′, A″) is the same for both tautomers of pyrrolide (1Na and 1Nb). Here, KT results produce a $\pi$-type HOMO (highest occupied molecular orbital), whereas all EPT calculations predict that the first VEDE for both anions corresponds to a $\sigma$-type orbital centered on the unhydrogenated carbon (HOMO-1 in Table 1). Previous KT calculations on the VEDEs of the pyrrolide anion produce an ordering of two $\pi$ holes followed by a nitrogen-localized $\sigma$ hole ($a_2$, $b_1$, $a_1$) that is confirmed by EPT refinements.[14] For all three structures, corrections to KT results are much larger for $\sigma$-hole states than for $\pi$-hole states, but only for the two tautomeric forms is the order of the final, doublet states altered by EPT calculations. The orbital pictures show that there is little participation from the nitrogen atom in the HOMO and HOMO-1. In the two tautomeric structures, the A′ Dyson orbitals are localized on the carbons without bonds to hydrogens. A higher A′ VEDE pertains to the case where this carbon has a neighboring NH group. The $\pi$ Dyson orbitals in the tautomeric forms bear some resemblance to their $a_2$ and $b_1$ counterparts in pyrrolide, with greater distortions taking place in the 1Nb case.

Table 2a displays results for the 2Na, 2Nb, and 2Nc imidazolide isomers. The VEDEs follows the same trend as the relative stability of these isomers (see Figure 2). As in the

**TABLE 1: Pyrrolide Tautomer VEDEs (eV) and Dyson Orbitals**

1Na

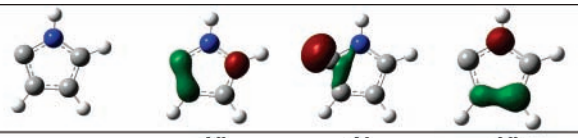

| | A" | A' | A" |
|---|---|---|---|
| KT | -1.956 | -3.237 | -3.949 |
| 2nd Order | -1.752 | -1.320* | -2.939 |
| 3rd Order | -2.250 | -2.473 | -3.807 |
| OVGF | -2.104 | -1.989 | -3.427 |
| P3 | -2.258 | -2.116 | -3.629 |
| P3+ | -2.166 | -1.944 | -3.495 |

1Nb

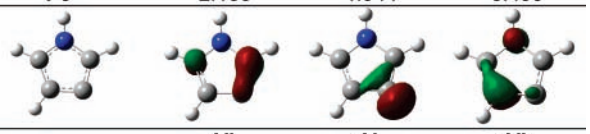

| | A" | A' | A" |
|---|---|---|---|
| KT | -2.283 | -2.478 | -3.502 |
| 2nd Order | -1.932 | -0.673* | -2.699 |
| 3rd Order | -2.571 | -1.939 | -3.493 |
| OVGF | -2.379 | -1.430 | -3.125 |
| P3 | -2.510 | -1.533 | -3.378 |
| P3+ | -2.401 | -1.350 | -3.247 |

[a] Pole strengths are between 0.80 and 0.85.

pyrrolide case, the order of HOMO and HOMO-1 predicted by KT is inverted when using electron propagator methods. Again, all EPT methods present lower VEDEs for the $\sigma$-type orbital (HOMO-1). Low-intensity features in a recent photoelectron spectrum have been assigned to the 2Na isomer, and the adiabatic electron affinity of the corresponding doublet radical was given as $1.992 \pm 0.010$ eV,[11] in good agreement with the P3+ VEDEs. In the reference imidazolide anion, the KT and EPT orderings of states are identical, with two, $\pi$-hole states ($b_1$ and $a_2$) followed by two, nitrogen-localized, $\sigma$-hole states.[14] All three of the A′ Dyson orbitals shown in Table 2a are localized on the carbons without bonds to hydrogen. Higher VEDEs are associated with neighboring NH groups. Nodal surfaces in the $\pi$ Dyson orbitals resemble those of their $b_1$ and $a_2$ antecedents in imidazolide.

Large EPT corrections to KT results also occur for the 2N′a isomer of pyrazolide in Table 2b. However, for isomers 2N′b and 2N′c, KT results predict the order of final states correctly. The P3+ prediction of the lowest VEDE is in good agreement with a recent experimental report of the radical's adiabatic electron affinity, $2.104 \pm 0.005$ eV.[12] In the same report, density functional estimates of the other tautomers' electron affinities are within 0.25 eV of the present P3+ predictions for the corresponding anion VEDEs. The $b_1$ and $a_2$ VEDEs in the reference pyrazolide anion are approximately equal and are followed, as in imidazolide, by two $\sigma$ levels.[14] The lowest VEDEs of all three tautomers have A′ symmetry, and the associated Dyson orbitals are localized on carbons without bonds to H atoms. As in imidazolide, the highest of these $\sigma$ VEDEs pertains to a structure in which this kind of carbon is next to an NH group. On the basis of the trends seen in the two diazoles (2N′b versus 2N′c and 2Na versus 2Nb), there is a small destabilizing effect of a neighboring N atom (without a bond to H) on the $\sigma$ VEDEs. Unlike the pyrazolide anion case, the two $\pi$ levels in each of the tautomeric forms are clearly separated in energy. Whereas there is some resemblance between the corresponding Dyson orbitals and their $b_1$ and $a_2$ counterparts in pyrazolide for the 2N′b and 2N′c forms; major rearrangements are seen in the 2N′a case.

**TABLE 2: Imidazolide (a) and Pyrazolide (b) Tautomer VEDEs (eV) and Dyson Orbitals**

**(a) Imidazolide**

2Na

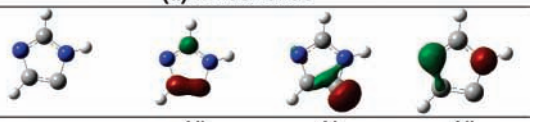

| | A" | A' | A" |
|---|---|---|---|
| KT | -2.314 | -3.567 | -5.224 |
| 2nd Order | -2.175 | -1.673* | -3.942* |
| 3rd Order | -2.636 | -2.810 | -4.979 |
| OVGF | -2.501 | -2.341 | 4.538 |
| P3 | -2.664 | -2.449 | -4.766 |
| P3+ | -2.577 | -2.285 | -4.607 |

2Nb

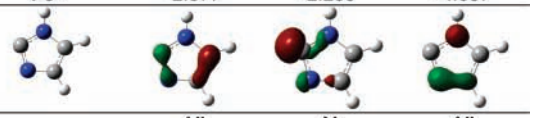

| | A" | A' | A" |
|---|---|---|---|
| KT | -2.683 | -3.387 | -4.975 |
| 2nd Order | -2.425 | -1.555* | -3.572* |
| 3rd Order | -2.956 | -2.660 | -4.792 |
| OVGF | -2.802 | -2.205 | -4.315 |
| P3 | -2.949 | -2.329 | -4.455 |
| P3+ | -2.856 | -2.170 | -4.281 |

2Nc

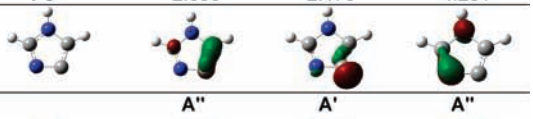

| | A" | A' | A" |
|---|---|---|---|
| KT | -2.517 | -2.599 | -4.929 |
| 2nd Order | -2.242 | -0.724* | -3.764* |
| 3rd Order | -2.827 | -2.036 | -4.804 |
| OVGF | -2.657 | -1.525 | -4.356 |
| P3 | -2.774 | -1.586 | -4.603 |
| P3+ | -2.677 | -1.402 | -4.439 |

**(b) Pyrazolide**

2N'a

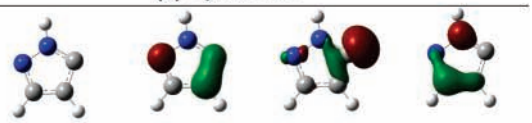

| | A" | A' | A" |
|---|---|---|---|
| KT | -3.080 | -3.709 | -4.323 |
| 2nd Order | -2.597 | -1.909* | -3.363 |
| 3rd Order | -3.194 | -2.896 | -4.226 |
| OVGF | -3.014 | -2.454 | -3.845 |
| P3 | -3.179 | -2.644 | -4.061 |
| P3+ | -3.074 | -2.491 | -3.928 |

2N'b

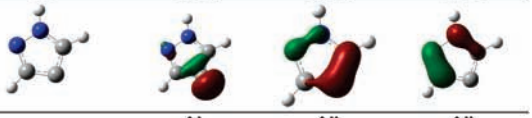

| | A' | A" | A" |
|---|---|---|---|
| KT | -2.986 | -3.107 | -4.124 |
| 2nd Order | -1.229* | -2.706 | -3.285 |
| 3rd Order | -2.331 | -3.296 | -4.089 |
| OVGF | -1.869 | -3.115 | -3.709 |
| P3 | -2.013 | -3.309 | -3.982 |
| P3+ | -1.850 | -3.198 | -3.848 |

2N'c

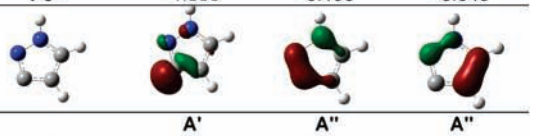

| | A' | A" | A" |
|---|---|---|---|
| KT | -2.660 | -3.512 | -3.788 |
| 2nd Order | -0.934* | -2.681* | -3.178 |
| 3rd Order | -2.089 | -3.679 | -3.814 |
| OVGF | -1.616 | -3.266 | -3.496 |
| P3 | -1.744 | -3.466 | -3.772 |

[a] Pole strengths are between 0.80 and 0.85.

**TABLE 3: 1,2,4 Triazolide (a) and 1,2,3 Triazolide (b) Tautomer VEDEs (eV) and Dyson Orbitals**

**(a) 1,2,4 Triazolide**

3Na

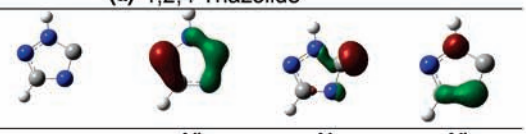

| | A" | A' | A" |
|---|---|---|---|
| KT | -3.976 | -3.985 | -5.370 |
| 2nd Order | -3.335 | -2.265 | -4.116 |
| 3rd Order | -4.070 | -3.184 | -5.163 |
| OVGF | -3.734 | -2.779 | -4.735 |
| P3 | -3.994 | -2.958 | -4.920 |
| P3+ | -3.875 | -2.819 | -4.767 |

3Nb

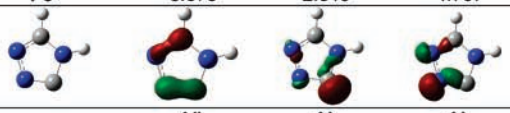

| | A" | A' | A' |
|---|---|---|---|
| KT | -3.605 | -3.842 | -5.656 |
| 2nd Order | -3.167 | -2.141 | -2.732* |
| 3rd Order | -3.876 | -3.158 | -5.149 |
| OVGF | -3.660 | -2.732 | -4.210 |
| P3 | -3.814 | -2.869 | -4.224 |
| P3+ | -3.696 | -2.722 | -3.874 |

3Nc

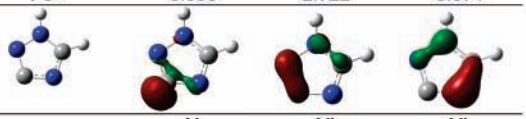

| | A' | A" | A" |
|---|---|---|---|
| KT | -3.104 | -3.872 | -5.296 |
| 2nd Order | -1.414 | -3.125 | -4.220* |
| 3rd Order | -2.510 | -4.047 | -5.150 |
| OVGF | -2.071 | -3.671 | -4.740 |
| P3 | -2.172 | -3.857 | -5.000 |
| P3+ | -2.018 | -3.720 | -4.852 |

**(b) 1,2,3 Triazolide**

3N'a

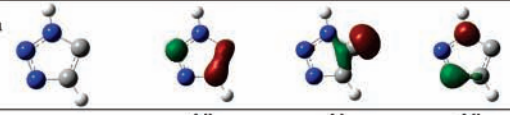

| | A" | A' | A" |
|---|---|---|---|
| KT | -3.380 | -4.240 | -5.597 |
| 2nd Order | -3.130 | -2.455 | -4.515* |
| 3rd Order | -3.531 | -3.408 | -5.392 |
| OVGF | -3.408 | -2.967 | -4.970 |
| P3 | -3.649 | -3.177 | -5.297 |
| P3+ | -3.557 | -3.026 | -5.146 |

3N'b

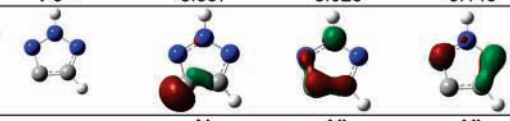

| | A' | A" | A" |
|---|---|---|---|
| KT | -3.297 | -3.812 | -4.960 |
| 2nd Order | -1.581 | -3.314 | -4.191* |
| 3rd Order | -2.589 | -3.924 | -4.937 |
| OVGF | -2.146 | -3.598 | -4.551 |
| P3 | -2.329 | -3.943 | -4.918 |
| P3+ | -2.175 | -3.827 | -4.779 |

3N'c

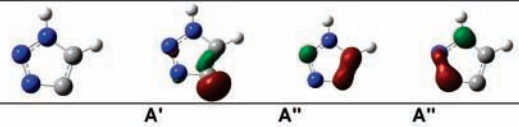

| | A' | A" | A" |
|---|---|---|---|
| KT | -3.156 | -3.381 | -5.384 |
| 2nd Order | -1.401* | -3.175 | -4.371* |
| 3rd Order | -2.541 | -3.610 | -5.236 |
| OVGF | -2.064 | -3.476 | -4.796 |
| P3 | -2.201 | -3.713 | -5.180 |
| P3+ | -2.033 | -3.617 | -5.020 |

[a] Pole strengths are between 0.80 and 0.85.

**TABLE 4: Tetrazolide Tautomer VEDEs (eV) and Dyson Orbitals**

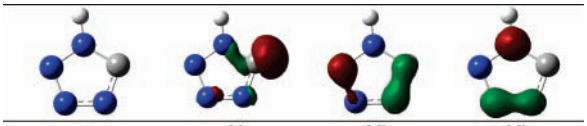

| | A' | A" | A" |
|---|---|---|---|
| KT | -4.600 | -4.639 | -6.258 |
| 2nd Order | -2.948 | -4.186 | -5.072 |
| 3rd Order | -3.834 | -4.731 | -5.995 |
| OVGF | -3.428 | -4.559 | -5.561 |
| P3 | -3.627 | -4.825 | -5.880 |
| P3+ | -3.491 | -4.709 | -5.724 |

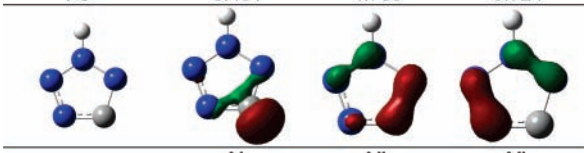

| | A' | A" | A" |
|---|---|---|---|
| KT | -3.767 | -4.483 | -6.058 |
| 2nd Order | -2.115 | -4.067 | -5.127* |
| 3rd Order | -3.128 | -4.635 | -5.869 |
| OVGF | -2.693 | -4.455 | -5.455 |
| P3 | -2.847 | -4.716 | -5.899 |
| P3+ | -2.698 | -4.599 | -5.750 |

[a] Pole strengths are between 0.80 and 0.85.

The tautomers of 1,2,4 triazolide presented in Table 3a show that the 3Na and 3Nb structures also have the reversed HOMO and HOMO-1 ordering problem at the KT level. VEDEs given by propagator methods for HOMO-1 are about 1 eV lower than those predicted by HOMO KT values. However, isomer 3Nc has a $\sigma$-type orbital as the HOMO, and the corresponding VEDE predictions with EPT methods are about 1.7 eV lower than those of HOMO-1. Table 3b depicts the 1,2,3 triazolide systems where the three nitrogen atoms are next to each other. Here, only 3N′a presents the HOMO and HOMO-1 reversal problem, while 3N′b and 3N′c binding energies are in the same order predicted by KT results. For each of the two reference triazolides, the two lowest VEDEs correspond to $\pi$-hole final states and are followed by three nitrogen-localized $\sigma$-hole states at the KT level.[14] P3+ results reverse the order of VEDEs for the second and third final states in the 1,2,4 case. Corrections to KT results bring the second through fourth final states within 0.1−0.2 eV of each other. For the tautomeric forms, the lowest VEDEs all have A′ symmetry and are localized on the carbon without a bond to a hydrogen atom. These values are largest for those cases where such carbons are next to an NH group. Considerable distortions of the $\pi$ Dyson orbitals with respect to those of 1,2,3 and 1,2,4 triazoles are obtained for the 3Na, 3Nc, 3′Nb, and 3′Nc structures. For the 3Nb case, the third VEDE belongs to a $\sigma$ Dyson orbital with large, opposite-phase amplitudes on N1 and N2.

Table 4 shows the results for tetrazolide isomers. In both tautomers of the tetrazolide, the HOMO is a $\sigma$ orbital centered on the carbon atom. EPT corrections to KT results are much larger for these levels than for the $\pi$ cases. In the reference tetrazolide anion, the first VEDE ($b_1$) corresponds to a $\pi$ Dyson orbital; one $\pi$ and four $\sigma$ levels lie at higher energies within 0.2 eV of each other.[14] The tautomeric isomer with the higher first VEDE has its carbon atom next to an NH group. Major distortions in the $\pi$ Dyson orbitals with respect to those of the reference tetrazolide are seen.

Some general trends for the azolide isomers may be discerned in the present results and those of our previous study.[14] Total energy differences between the most stable structures and the

lowest tautomeric isomers are quite large and vary between 32 and 55 kcal/mol. Despite their relative instability, these tautomeric species may be produced for the purpose of spectroscopic interrogation by chemical reactions between precursor molecules and strong bases in the gas phase. The lowest VEDEs of the tautomeric forms correspond to $\sigma$-hole, final-state doublets whose Dyson orbitals are localized on carbon atoms without bonds to hydrogen neighbors. KT predictions may err on this point, and correlated EPT corrections are frequently needed to set the correct order of final states. VEDEs associated with $\sigma$ Dyson orbitals of this type are larger when there is an NH group next to the carbon without a bond to a hydrogen atom. A smaller but opposite trend in $\sigma$ VEDEs accompanies proximity of such carbons to nitrogen atoms without bonds to hydrogen atoms. Higher VEDEs belong to $\pi$-hole, final-state doublets. This ordering contrasts with that seen for the reference anions,[14] where the lowest VEDE corresponds to a $\pi$-hole, final-state doublet. In the reference anions and in the tautomeric forms, corrections to KT results are considerably larger for $\sigma$-hole states than for $\pi$-hole states. Whereas orbital relaxation and correlation effects are strong for cases where a $\sigma$ Dyson orbital is localized on a carbon without bonds to hydrogens, the description of the change in electronic structure that accompanies electron detachment provided by KT remains qualitatively valid.

## IV. Conclusions

The present study is an extension of our previous paper[14] on polynitrogen pentagonal aromatic anions. Tautomeric forms for each anion have been characterized, and their vertical electron detachment energies have been determined using electron propagator theory. We find many unforeseeable similarities among these isomers. Probably the most remarkable conclusion is that standard Hartree−Fock calculations do not describe the lowest VEDE correctly in many of these aromatic systems. Whereas Koopmans's theorem results are not reliable, correlated electron propagator calculations correctly predict the order of the two lowest VEDEs in all cases. This conclusion underscores the need for incorporating correlation and orbital relaxation in calculations of electron detachment energies, and the electron propagator decouplings utilized here provide a means to this end.

**Acknowledgment.** The National Science Foundation provided support through Grant CHE-0451810 to Auburn University. M.K.M. is pleased to acknowledge support from DST Grant SR/S1/PC-30/2006 to IIT Bombay.

## References and Notes

(1) Fau, S.; Wilson, K. J.; Bartlett, R. J. *J. Phys. Chem. A* **2002**, *106*, 4639.

(2) Gagliardi, L.; Orlandi, G.; Evangelisti, S.; Roos, B. O. *J. Chem. Phys.* **2001**, *114*, 10733.

(3) Nguyen, M. T.; Ha, T. K. *Chem. Phys. Lett.* **2001**, *335*, 311.

(4) Vianello, R.; Maksic, Z. B. *Mol. Phys.* **2005**, *103*, 209.

(5) Vij, A.; Wilson, W. W.; Vij, V.; Tham, F. S.; Sheehy, J. A.; Christe, K. O. *J. Am. Chem. Soc.* **2001**, *123*, 6308.

(6) Vij, A.; Pavlovich, J. G.; Wilson, W. W.; Vij, V.; Christe, K. O. *Angew. Chem., Int. Ed.* **2002**, *41*, 3051.

(7) Butler, R. N.; Stephens, J. C.; Burke, L. A. *Chem. Commun.* **2003**, 1016.

(8) Ostrovskii, V. A.; Brusalimskii, G. B.; Shcherbinin, M. B. Z. *Org. Khimi* **1995**, *31*, 1422.

(9) Moore, D. S.; Robinson, S. D. *Adv. Inorg. Chem.* **1988**, *32*, 171.

(10) Gianola, A. J.; Ichino, T.; Hoenigman, R. L.; Kato, S.; Bierbaum, V. M.; Lineberger, W. C. *J. Phys. Chem. A* **2004**, *108*, 10326.

(11) Gianola, A. J.; Ichino, T.; Hoenigman, R. L.; Kato, S.; Bierbaum, V. M.; Lineberger, W. C. *J. Phys. Chem. A* **2005**, *109*, 11504.

(12) Gianola, A. J.; Ichino, T.; Kato, S.; Bierbaum, V. M.; Lineberger, W. C. *J. Phys. Chem. A* **2006**, *110*, 8457.

(13) Ichino, T.; Gianola, A. J.; Lineberger, W. C.; Stanton, J. F. *J. Chem. Phys.* **2006**, *125*, 084312.

(14) Melin, J.; Mishra, M. K.; Ortiz, J. V. *J. Phys. Chem. A* **2006**, *110*, 12231.

(15) Da Silva, G.; Moore, E. E.; Bozzelli, J. W. *J. Phys. Chem. A* **2006**, *110*, 13979.

(16) Linderberg, J.; Öhrn, Y. *Propagators in Quantum Chemistry*, 2nd ed.; Wiley: Hoboken, New Jersey, 2004.

(17) Ortiz, J. V. *Adv. Quantum Chem.* **1999**, *33*, 35.

(18) Mishra, M. K.; Medikeri, M. N. *Adv. Quantum Chem.* **1996**, *27*, 225.

(19) Ferreira, A. M.; Seabra, G.; Dolgounitcheva, O.; Zakrzewski, V. G.; Ortiz, J. V. In *Quantum-Mechanical Prediction of Thermochemical Data;* Cioslowski, J., Ed.; Kluwer: Dordrecht, 2001; p 131.

(20) Ortiz, J. V. In *Computational Chemistry: Reviews of Current Trends*, Vol. 2; Leszczynski, J., Ed.; World Scientific: Singapore, 1997; p 1.

(21) Venkatnathan, A.; Mahalakshmi, S.; Mishra, M. K. *J. Chem. Phys.* **2001**, *114*, 35.

(22) Mahalakshmi, S.; Venkatnathan, A.; Mishra, M. K. *J. Chem. Phys.* **2001**, *115*, 4549.

(23) Ortiz, J. V. *Int. J. Quantum Chem.* **2005**, *105*, 803.

(24) Frisch, M. J.; Trucks, G. W.; Schlegel, H. B.; Scuseria, G. E.; Robb, M. A.; Cheeseman, J. R.; Montgomery, J. A., Jr.; Vreven, T.; Kudin, K. N.; Burant, J. C.; Millam, J. M.; Iyengar, S. S.; Tomasi, J.; Barone, V.; Mennucci, B.; Cossi, M.; Scalmani, G.; Rega, N.; Petersson, G. A.; Nakatsuji, H.; Hada, M.; Ehara, M.; Toyota, K.; Fukuda, R.; Hasegawa, J.; Ishida, M.; Nakajima, T.; Honda, Y.; Kitao, O.; Nakai, H.; Klene, M.; Li, X.; Knox, J. E.; Hratchian, H. P.; Cross, J. B.; Bakken, V.; Adamo, C.; Jaramillo, J.; Gomperts, R.; Stratmann, R. E.; Yazyev, O.; Austin, A. J.; Cammi, R.; Pomelli, C.; Ochterski, J. W.; Ayala, P. Y.; Morokuma, K.; Voth, G. A.; Salvador, P.; Dannenberg, J. J.; Zakrzewski, V. G.; Dapprich, S.; Daniels, A. D.; Strain, M. C.; Farkas, O.; Malick, D. K.; Rabuck, A. D.; Raghavachari, K.; Foresman, J. B.; Ortiz, J. V.; Cui, Q.; Baboul, A. G.; Clifford, S.; Cioslowski, J.; Stefanov, B. B.; Liu, G.; Liashenko, A.; Piskorz, P.; Komaromi, I.; Martin, R. L.; Fox, D. J.; Keith, T.; Al-Laham, M. A.; Peng, C. Y.; Nanayakkara, A.; Challacombe, M.; Gill, P. M. W.; Johnson, B.; Chen, W.; Wong, M. W.; Gonzalez, C.; Pople, J. A. *Gaussian 03*, revision B.03; Gaussian, Inc.: Wallingford, CT, 2003.

(25) Von Niessen, W.; Schirmer, J.; Cederbaum, L. S. *Comp. Phys. Rep.* **1984**, *1*, 57.